INSTABILITIES AND TRANSITION IN HIGH VELOCITY RATIO COAXIAL JETS: A NUMERICAL STUDY

Carlos B. da Silva*, Guillaume Balarac, Patrick Begou, Olivier Métais
Equipe MoST/LEGI, Institut de Mécanique de Grenoble,
B.P. 53, 38041 Grenoble Cedex 09, France
csilva@hmg.inpg.fr,balarac@hmg.inpg.fr, begou@hmg.inpg.fr, metais@hmg.inpg.fr

ABSTRACT

Direct Numerical Simulations (DNS) are performed to analyze the instability, transition scenario and resulting topology from high velocity ratio coaxial jets ($r_u = 3.3$ and $r_u = 23.5$). The inner and outer shear layers roll up into axissymmetric vortex rings due to the Kelvin-Helmholtz instability. For $r_u = 3.3$ the outer primary vortices evolve according to the theory considering an isolated mixing layer profile, and impose their evolution upon the inner structures which are 'locked' into the outer ones. For $r_u = 23.5$ there is a big recirculation region which affects only lightly the development of the Kelvin-Helmholtz instabilities. The preferred mode for simple (non-coaxial) round jets is well recovered at the end of the potential core region in the case $r_u = 3.3$ but not when $r_u = 23.5$ due to the presence of the backflow region. The structure of the preferred mode is the same in both cases, however, and consists in an helical arrangement ($m = 1$). Finally, when the bubble is present one can see that the inner streamwise structures, corresponding to the secondary instabilities, are stretched by the presence of the bubble which acts as an additional source of axial vorticity production.

INTRODUCTION

Coaxial jet flows are often used in industrial applications as an effective way of mixing two different fluid streams (*e.g.* mixing air and combustible in jet engines). A coaxial jet is made when a fluid stream with velocity U_2, issuing from an outer annulus of diameter D_2, is added into a round jet flow with velocity U_1, and (inner) nozzle diameter D_1 ($D_1 < D_2$). Annular jets correspond to the case when there is no inner fluid stream, $U_1 = 0$.

The existence of two (inner and outer) shear layer regions in coaxial jets was evidenced by Ko and Kwan (1976) and Kwan and Ko (1977) through the observation of two different peak spectrum frequencies corresponding to the passing frequencies of vortices originated in the inner and outer shear layers. They noticed also the formation of two potential cores, corresponding to each one of these regions. In their case ($U_2 < U_1$ and U_2 relatively small) the outer stream acts mainly as a co-flowing velocity which does not modify substantially the inner jet dynamics.

Dahm *et al.* (1992) highlighted the importance of the initial outer to inner velocity ratio $r_u = U_2/U_1$, in the selection of the several existing flow regimes. For low initial velocity ratios ($0.59 < r_u < 0.71$) the outer shear layer instability rolls up into axisymmetric vortex rings ($m = 0$) that turn further downstream into an helical shaped structure ($m = 1$), in agreement with the linear stability theory results for a single jet flow. These primary rings travel downstream at a frequency which agrees well with the value predicted by the linear stability theory considering an initial "wake + mixing layer" velocity profile. The inner shear layer, on the other hand, has a lethargic behavior and never rolls up into vortical structures before being dominated by the helical vortices from the outer layer. But for large initial velocity ratios ($r_u = 2.56$) the inner shear layer also develops into ring shaped vortices which interact with the outer vortex structures. One of the most important results from this study was the observation of a "locking" phenomena between the two shear layers. It was observed that the vortex passage frequency from the inner shear layer differs from the value predicted by the stability analysis of a single shear layer with the same characteristics. The reason for this comes from the fact that the vortices from the inner shear layer are trapped into the free spaces left between two consecutive outer layer vortices. The latter modify the "normal" inner shear layer development which is in this way "locked" into the outer layer dynamics. Another important observation is related to the initial vorticity thickness of the initial inner and outer shear layers. It was observed that for the same initial velocity ratio ($r_u = 1.0$), but using different absolute velocities, a dramatically different flow topology can be obtained. The reason for this can be found in the difference in the initial shear layer thicknesses. In general, smaller initial vorticity thicknesses lead to a faster roll up process (for the same velocity jump), thus causing very different flow topologies.

The influence of the velocity ratio r_u in the flow regimes of coaxial jets was also analyzed by Rehab *et al.* (1997). They considered only $r_u > 1$ cases and found the existence of a critical velocity ratio r_{uc} above which the flow develops a big reverse flow region. The value of r_{uc} depends on the shape of the inlet velocity profiles (nozzle shape) and varies between about $5 < r_{uc} < 8$. A big recirculation bubble is always present in annular jets, which can be viewed as coaxial jets with $r_u = U_2/U_1 = \infty$ (Ko and Chan, 1979). For smaller than critical velocity ratios ($1 < r_u < r_{uc}$) the structures from the fast stream "pinch" the central jet at the end of the potential core x_{1p}. The pinching frequency is equal to the outer jet mode, $fD_2/U_2 \approx 0.4$. The value of x_{1p} decreases with increasing r_u. For greater than critical velocity ratios ($r_u > r_{uc}$) a large recirculating bubble forms with a size of the order of the inner diameter D_1 and which grows with increasing velocity ratio, r_u. One of the more interesting features of this back-flow region is the fact that it oscillates and rotates with the same frequency in a pure precession mode (m=1). This frequency is fixed by D_1 and U_2 and is one order of magnitude smaller than the original Kelvin-Helmholtz instability mode.

Numerical studies of coaxial jets are very rare and are

*Present address: Faculdade de Engenharia, Universidade do Porto, DEMEGI, Secção de Fluidos e Calor, Rua Dr. Roberto Frias, 4200-365 Porto, Portugal, cbsilva@fe.up.pt

often restricted to 2D cases, due to the need of massive computer resources. Among the limited number of numerical works on coaxial jets are the works of Akselvoll and Moin (1996) who studied co-annular jets by large-eddy simulations in a fully developed turbulent configuration. Salvetti (1996) made direct numerical simulations of axisymmetric (2D) coaxial jets to analyze the effects of the inlet condition on the dynamics of the vortical structures. Salvetti (2000) studied numerically the effect of inner/outer mutual interactions. It was observed that vortical inner/outer interactions tend to increase with increasing velocity ratio r_u. Finally, da Silva and Métais (2001) carried what is maybe the first direct numerical simulation of a coaxial jet, in order to study the flow topology in an excited (*varicose*) configuration.

The present work uses Direct Numerical Simulations (DNS) to analyze the instability, transition scenario and resulting topology from high velocity ratio coaxial jets. The approach and main results of this study have also been described in da Silva *et al.* (2003).

NUMERICAL METHOD

All the simulations presented here were performed with a code that solves the full, three-dimensional, incompressible Navier-Stokes equations. The code is a finite-difference solver that uses both 6^{th} order "Compact" and pseudo-spectral schemes for spatial discretization. Pressure-velocity coupling is assured by a fractional step method, requiring the solution of a Poisson equation to insure incompressibility of the velocity field. A 3 step, 3^{rd} order Runge-Kutta scheme is used for temporal discretization. As inlet boundary condition, each time step a given velocity profile is prescribed at the inlet, the details of which will be given in the next section. The outlet boundary condition is of non-reflective type. Full numerical discretization details can be found in da Silva (2001). The code was parallelized using the PVM library and the calculations were carried out on a ten nodes Linux Beowulf cluster.

DIRECT NUMERICAL SIMULATIONS OF COAXIAL JETS

Two Direct Numerical Simulations (DNS) were carried out (DNS1, DNS2). In both cases the shape of the inlet velocity profile is,

$$\vec{U}(\vec{x_0},t) = \vec{U}_{med}(\vec{x_0}) + \vec{U}_{noise}(\vec{x_0},t), \qquad (1)$$

where $\vec{U}(\vec{x_0},t)$ is the instantaneous inlet velocity vector, which is prescribed as inlet condition, for each time step. In equation (1) $\vec{U} = (U,V,W)$, where U,V and W are the streamwise, normal and spanwise velocities, respectively. We will also use the cylindrical coordinates $\vec{U} = (u_x, u_r, u_\theta)$, where u_x, u_r and u_θ represent the axial, radial and tangential velocity components, respectively.

One of the main difficulties in the numerical simulation of coaxial jets results from the complexity of the inlet velocity profile which has to be accurately represented. As stressed by Dahm *et al.* (1992), each one of the two shear layers can be described as a combined "wake + mixing layer" profiles. But, has shown by Rehab *et al.* (1997), the "wake" part of the mean streamwise velocity profiles disappears very fast. In the experimental measurements by Rehab *et al.* (1997) one can notice that all the "wake" part of the velocity profile disappears much before $x/D_1 = 1$. Therefore, it seems that an inlet velocity profile made up with two "hyperbolic tangent" velocity profiles could be a good approximation to the "real" velocity profile. In addition to this, this will allow a rigorous definition of the governing global parameters. This was the methodology adopted in the present study. The mean velocity profile is therefore represented as,

$$U_{med}(\vec{x_0}) = \begin{cases} \frac{U_1+U_2}{2} + \frac{U_1-U_2}{2}\tanh\left(\frac{r-R_1}{2\theta_{01}}\right) & \text{for } r < R_m \\ \frac{U_2+U_3}{2} + \frac{U_2-U_3}{2}\tanh\left(\frac{r-R_2}{2\theta_{02}}\right) & \text{for } r > R_m \end{cases}$$

Here U_1 is the inner coaxial jet velocity, U_2 is the outer velocity and U_3 is a very small co-flow. R_1, R_2 and $R_m = (R_1 + R_2)/2$ are the inner, outer and mean radius, and θ_{01} and θ_{02} are the initial momentum thicknesses from the inner and outer shear layers, respectively.

$\vec{U}_{noise}(\vec{x_0},t)$ is the inlet noise profile which is given by,

$$\vec{U}_{noise}(\vec{x_0},t) = A_n\ U_{base}(\vec{x_0})\vec{f}^{\,\prime}. \qquad (2)$$

A_n is the maximum amplitude of the incoming noise and $U_{base}(\vec{x_0})$ is a function that sets the noise location mainly in the shear layer gradients.

$\vec{f}^{\,\prime}$ is a random noise designed to satisfy a given energy spectrum. Note that the random noise is imposed on the three velocity components.

Both simulations were carried out on the same grid which consists in $231 \times 256 \times 256$ points and allows a domain size of $10.8D_1 \times 7.1D_1 \times 7.1D_1$, along the streamwise ($x$) and the two transverse directions (y,z), respectively. The mesh size is uniform in all three directions. In both simulations the Reynolds number and the ratio of outer to inner diameters was $Re_{D_1} = \frac{U_2 D_1}{\nu} = 3000$ and $\beta = \frac{D_2}{D_1} = 2$, respectively. The ratio of the jet radius to the initial shear layer momentum thicknesses was $\frac{R_1}{\theta_{01}} = \frac{R_2}{\theta_{02}} = 13$ and the maximum noise amplitude was limited to $A_n = 4.0\%$.

The difference between the two simulations concerns the initial velocity ratio $r_u = U_2/U_1$. In the first simulation (DNS1), this ratio was set to $r_u = U_2/U_1 = 3.3$. The second simulation (DNS2) uses $r_u = U_2/U_1 = 23.5$.

RESULTS AND DISCUSSION

Figures 1 (a) and (b) show instantaneous fields of positive Q criteria (Hunt *et al.*, 1988). The main features of both flows can be appreciated here. In the early transition stages ($x/D_1 < 2$), both the inner and outer shear layers roll up into vortex rings that turn in opposite sense, due to the Kelvin-Helmholtz instability created by the shape of the initial velocity profiles. The rings seem to preserve the same wave-length spacing λ_0, until $x/D_1 \approx 7$ where they begin to appear less clear due the growth of small scale turbulence. Around the middle of the computational domain $x/D_1 \approx 7$, pairs of streamwise vortices appear between two consecutive outer rings, in agreement with the classical scenario of transition in free shear layers. Further downstream, just before the end of the computational domain, the growth of small scale turbulence near the structures as well as the typical processes of fragmentation and tearing, turns the identification of the coherent structures very difficult. By $x/D_1 \approx 8$ the structures no longer exhibit any preferential direction and seem 'isotropic', an indication that the flow is quickly reaching a state of fully developed turbulence (axial velocity spectra taken from this region exhibit a $-5/3$ range over about one decade).

Figures 2 (a) and (b) show contours of streamwise velocity for both simulations. There is a strong back-flow region in DNS2 which can be seen through isosurfaces of negative axial velocity $u_x(x,r)$, The recirculation bubble is centered at $x/D_1 \approx 2.5$ (see figure 2 (b)). Around this location the

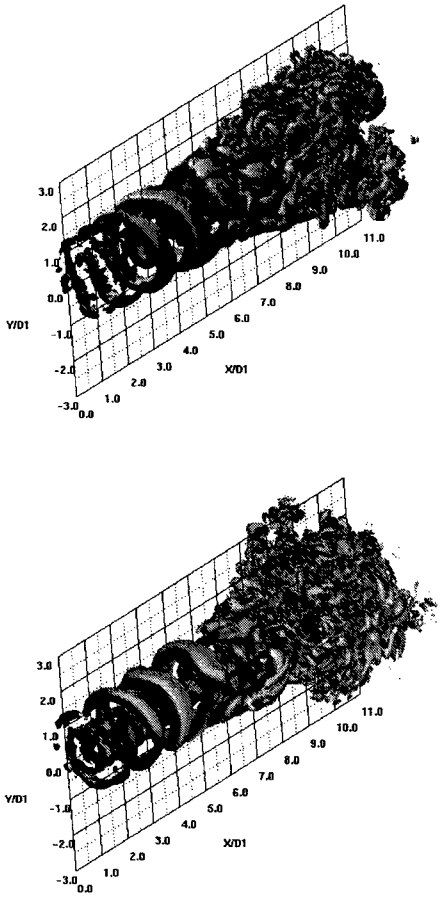

Figure 1: Isosurfaces of positive Q criteria in DNS1 (top); and DNS2 (bottom).

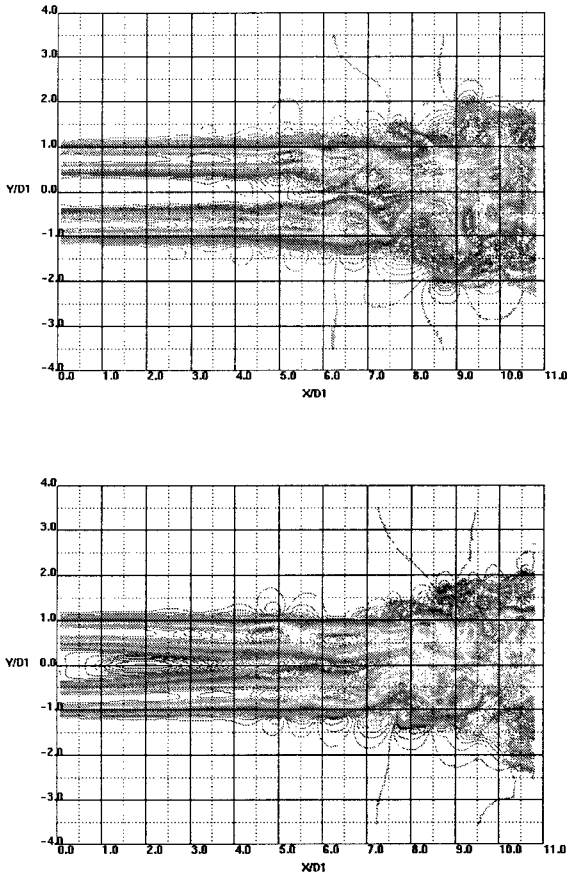

Figure 2: Contours of streamwise velocity $u_x(x,r)$, in DNS1 (top); and DNS2 (bottom). The contour lines are in a slice which passes through the plane $(x,y,z=0)$.

flow evolves smoothly, therefore indicating that the recirculation bubble is either stationary or evolving slowly, since it seems to be surrounded by laminar flow. It is interesting to note also the downstream evolution of the two outer shear layers (*i.e.* the two layers of maximum streamwise velocity, starting at $r/D_1 = 0.5$). Whereas in DNS1 (no recirculation bubble) the outer shear layer thickness grows as the flow evolves downstream, in DNS2 the two outer streams converge after the back-flow region, leading to a decrease in the overall shear layer thickness at $x/D_1 \approx 7$.

Finally, an interesting feature could be seen in the instantaneous iso-surfaces of vorticity norm (not shown). These figures showed that the evolution of the inner and outer layers is not independent, but the vortices from the inner shear layer are trapped into the free spaces between two consecutive outer layer vortices. Moreover, one could also observe a 'pinching' mechanism when the inner and outer streams plunge into the centerline. Similar observations were made in experimental coaxial jets by Rehab *et al.* (1997).

One point statistics for DNS1 (not shown) showed that in DNS1 the axial velocity is constant in a region extending to $l^{in}_{core} \approx 5D_1$ at the centerline ($r = 0$) and $l^{out}_{core} \approx 5D_1$ at the center of the outer jet ($r = R_m$). This shows that in DNS1, two potential core regions exist, one at the inner and another at the outer jet. In DNS2 (figure 3) the outer jet also exhibits a potential core region, with length $l^{out}_{core} \approx 6D_1$, but the same does not occur in the inner jet. Here the centerline axial velocity is negative between $x/D_1 \approx 0.5$ and $x/D_1 \approx 4.0$, due to the presence of the back-flow region. The axial length of this structure is $l_{bx} \approx 3.5D_1$.

Table 1: Strouhal numbers of the most amplified modes in the outer (o) and inner (i) shear layers for simulations DNS1 and DNS2. The spectra were computed using time series of the streamwise velocity component located at $(r/D_1, x/D_1) = (1,3)$ (outer layer) and $(r/D_1, x/D_1) = (0.5,3)$ (inner layer).

Simulation	Str^o_θ	Str^i_θ
DNS1	0.028	0.011
DNS2	0.030	0.010

Primary instabilities: jet shear layer mode

In order to see whether each (inner/outer) shear layer evolves according to the Kelvin-Helmholtz instability theory, we computed time spectra from the streamwise velocity signal at two locations. All spectra show peaks at a given Strouhal number. The results are listed in table 1.

Here we see that whereas the outer shear layer instabilities agree very well with the theoretical value ($Str_{\theta_0} = 0.033$ - Gutmark and Ho, 1983), the inner shear layers do not. A possible explanation for this fact can be gained by looking into the values of the actual frequencies as shown in table 2.

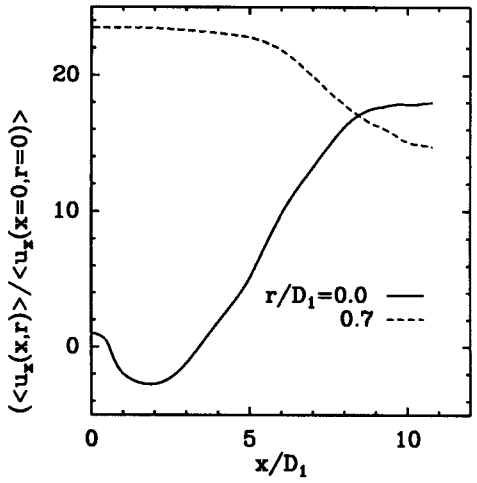

Figure 3: Downstream evolution of the axial velocity component at $r/D_1 = 0$ and $r/D_1 = 0.75$ for DNS2.

Table 2: Frequencies $f_* = fD_1/2U_2$ of the most amplified modes in the outer (o) and inner (i) shear layers for simulations DNS1 and DNS2. The frequencies are the same displayed in table 1.

Simulation	f_*^o	f_*^i
DNS1	0.40	0.40
DNS2	0.45	0.30

This table shows that for DNS1 (no recirculation bubble), the inner and outer frequencies are exactly the same. This suggests that the outer shear layer grows according to the theory (without 'feeling' the inner shear layer) and then imposes its evolution upon the inner shear layer, thus causing the inner/outer shear layers 'locking' described before.

The fact that the outer shear layer is dominating the inner layer can be explained in a number of ways. In DNS1 the initial vorticity of the outer shear layer is much bigger than the inner one (see the initial inner and outer velocity ratios) which not only causes the outer vortex rings to appear sooner than the inner ones, (see figure 5 (a) below) but creates also outer rings with total vorticity which is higher than the total vorticity associated with the inner rings.

This is likely to make the outer vortices dominant over the inner rings through inviscid vorticity induction (Biot-Savart), and therefore explains that the evolution of the inner structures is dictated by the motion of the outer, more important structures.

Things are more complicated in DNS2 due to the back-flow region. In this case the inner structures are not convected at the same speed of the outer ones, as can be assessed by the different values of their dimensional frequencies (see table 2). One possible explanation is that the back-flow region, being so close to the inner rings, will turn to decrease

Table 3: Strouhal numbers of the most amplified modes at the end of the potential cores for DNS1 and DNS2, in the outer (o) and inner (i) shear layers. The spectra were computed using time series of the streamwise velocity component located at $(r/D_1, x/D_1) = (0.75, 6)$ (outer layer) and $(r/D_1, x/D_1) = (0, 6)$ (inner layer).

Simulation	Str_D^o	Str_D^i
DNS1	0.40	0.60
DNS2	5.0	5.0

their traveling speed, thus making $f_*^i < f_*^o$ in this case. This phenomena should be investigated with greater depth in future works.

To compare the evolution of the inner and outer shear layers, it is instructive to look into the downstream evolution of the following quantities:

$$E_r^i(x) = \sqrt{\frac{2\pi}{L_y L_z} \int_0^{R_m} < u_r'^2(x,r) > r dr} \qquad (3)$$

$$E_\theta^i(x) = \sqrt{\frac{2\pi}{L_y L_z} \int_0^{R_m} < u_\theta'^2(x,r) > r dr} \qquad (4)$$

$$E_r^o(x) = \sqrt{\frac{2\pi}{L_y L_z} \int_{R_m}^{\infty} < u_r'^2(x,r) > r dr} \qquad (5)$$

$$E_\theta^o(x) = \sqrt{\frac{2\pi}{L_y L_z} \int_{R_m}^{\infty} < u_\theta'^2(x,r) > r dr} \qquad (6)$$

In the above, $E_r(x)$ and $E_\theta(x)$, are the contribution of the radial and azimuthal Reynolds stresses to the turbulent kinetic energy at a given x location, respectively. The superscripts i and o define the inner and outer shear layers.

The downstream evolution of these quantities confirms the previous observations, showing that the outer instabilities begin to grow first than the inner ones and dominate the whole transition region (*i.e.* $E_r^o(x) > E_r^i(x)$ and $E_\theta^o(x) > E_\theta^i(x)$) in DNS1 and DNS2 (figure 4).

Primary instabilities: jet preferred mode

In simple (non-coaxial) jets one speaks often in the so-called *Preferred* jet mode which characterizes virtually all round jets, at sufficiently high Reynolds numbers. The frequency of the Preferred jet mode is the frequency at which the vortex rings cross the end of the potential core and corresponds to a Strouhal number which is $0.24 < Str_D = fD/U_0 < 0.5$ (Gutmark and Ho, 1983). It has been observed experimentally that coaxial jets also display this Preferred jet frequency at the end of the central potential core (Rehab *et al.*, 1997). Therefore, it is interesting to see weather the same happens in the present case. For this purpose table 3 shows the Strouhal numbers of the most unstable modes found at the end of the inner and outer potential cores for DNS1 and DNS2.

The table shows that for DNS1, the preferred mode is well recovered in the outer shear layer, but not in the inner layer. Since the preferred mode follows the evolution of the shear layer mode, this fact can be explained as before: the outer vortex rings being more important, evolve according to the theory and impose their evolution on the

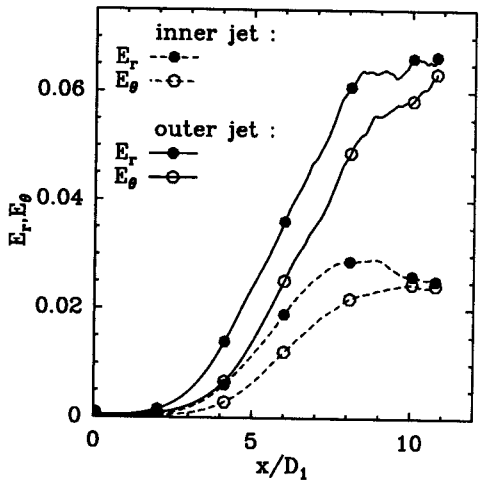

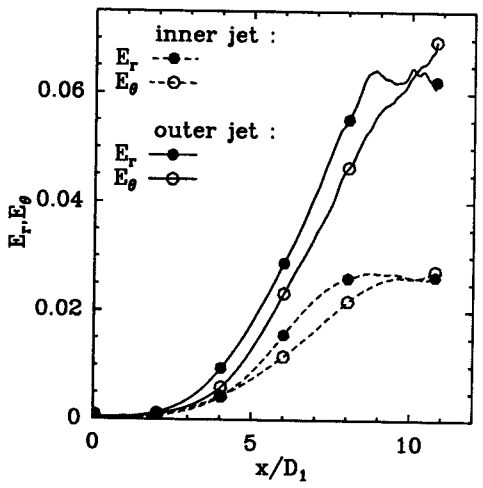

Figure 4: Downstream evolution of the radial, E_r (equations 3 and 5) and tangential E_θ (equations 4 and 6) contributions for the total kinetic energy in the inner (i) and outer (o) shear layers. DNS1 (top); DNS2 (bottom).

inner ones. As discussed before the same applies to the evolution of DNS2, although in this case, the preferred mode is not well recovered. The value $Str_D^i = 5$ falls by far outside the accepted range cited before. One way to explain this is through the quick convergence of the streamlines just after the recirculation bubble. The inner structures will have to cross in that case, a much smaller section, which explains their acceleration (and higher passing frequency). Furthermore, these structures, being stretched in this way, will tend to increase their axial vorticity level, thus increasing also the level of small scale turbulence within themselves. It was observed, in agreement with this explanation, that in DNS2, unlike DNS1, the spectra show a range of high frequencies, rather then a given distinct peak (table 3 shows only the frequency corresponding to the higher energy). This point will be further discussed below.

The structure of the preferred mode can be studied in figure 5 showing isosurfaces of positive Q colored by the streamwise vorticity for DNS1 and DNS2. The outer vortices are organized into a single helix type structure. One speaks in an *Helical* arrangement of mode $m = 1$. The inner structures have the same arrangement (figure 5) and both helixes (inner/outer) turn in the same direction in each case. These observations agree with the theoretical results for the preferred mode considering a single round jet. Indeed, Cohen and Wygnanski (1987) showed that the ratio R/θ dictates the structure resulting from the preferred mode at the end of the potential core. For $R/\theta > 6.5$ axisymmetric structures are formed (vortex rings). For $R/\theta < 6.5$ helical-like structures appear. In the present cases R/θ is indeed below 6.5 at the end of the potential cores.

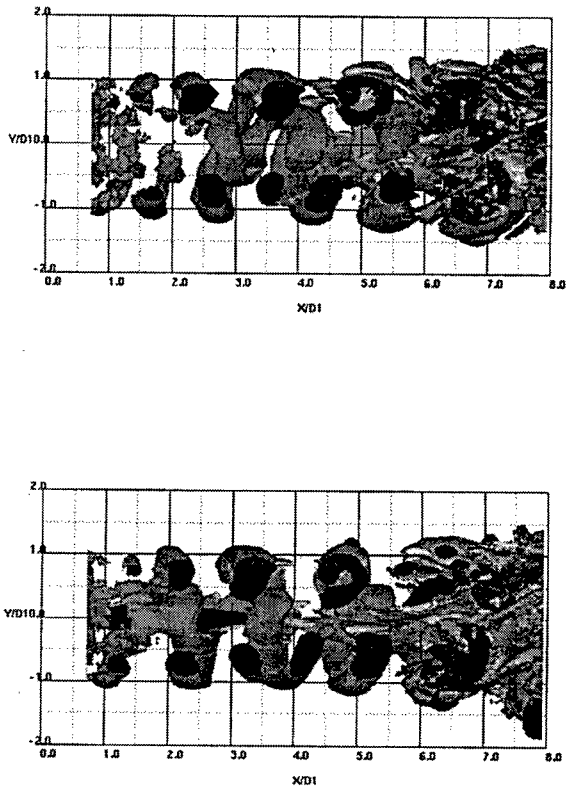

Figure 5: Cut view of positive Q isosurfaces colored by the streamwise vorticity in DNS1 (top); DNS2 (bottom).

Secondary instabilities

In the classical transition scenario for simple (non-coaxial) round jets, once the rings have been formed, one observes usually the emergence of a wavy structure along the azimuthal direction in each vortex ring. Unlike the

forced coaxial jets observed by da Silva and Métais (2001), it is very difficult to discern an azimuthal perturbation in the rings from DNS1 and DNS2. Indeed, the primary rings show very little sign of any azimuthal perturbation in their shape. This agrees with what we can see in figures 4 (a) and (b). In DNS1 and DNS2, $E_r(x)$, associated with the growth of the vortex rings, dominates $E_\theta(x)$, associated with the growth of the azimuthal perturbations $E_r(x) > E_\theta(x)$, until about $x/D_1 \approx 10$ where $E_r(x) \approx E_\theta(x)$. It seems than the growth of the vortex rings is dominating the evolution of the other instabilities until quite late in the transition process ($x/D_1 \approx 10$).

In DNS2 the presence of a back-flow region decreases the degree of domination of $E_r(x)$ over $E_\theta(x)$, *i.e.*, $|E_r^i(x) - E_\theta^i(x)|_{DNS2} < |E_r^i(x) - E_\theta^i(x)|_{DNS1}$, and $|E_r^o(x) - E_\theta^o(x)|_{DNS2} < |E_r^o(x) - E_\theta^o(x)|_{DNS1}$. The recirculation bubble acts then as a 'destabilizing' effect in this predominance of the vortex rings in the transition mechanism.

Concerning the streamwise vortices, there is an interesting difference between DNS1 and DNS2. As discussed before, just after the back-flow region in DNS2 ($x/D_1 > 6.5$) the streamwise inner vortices not only appear much sooner than in DNS1, but are particularly elongated (figure 5 (a)). Furthermore, these inner structures are characterized by extremely high values of vorticity. It is possible to explain these observations considering the production term in the axial vorticity equation,

$$P_{(\Omega_x)} = \Omega_x \frac{\partial u_x}{\partial x} + \Omega_y \frac{\partial u_x}{\partial y} + \Omega_z \frac{\partial u_x}{\partial z}. \qquad (7)$$

As in other flows with a recirculation bubble, in the region just after it there is an high streamwise velocity gradient, $\partial u_x/\partial x$. In the coaxial jet flow, this region is where the streamwise vortices begin to develop, and therefore, contributes to create axial vorticity, Ω_x, by vortex stretching of the inner streamwise vortices, $\Omega_x \frac{\partial u_x}{\partial x}$. Thus, the back-flow region creates an additional source of axial vorticity production. A similar observation was made by da Silva and Métais (2001) in a DNS of a forced coaxial jet with a back-flow region.

CONCLUSIONS

In the present work two Direct Numerical Simulations (DNS1, DNS2) were carried out in order to analyze the instabilities and transition in high velocity ratio coaxial jets ($r_u = 3.3$ and $r_u = 23.5$). In DNS1 two potential core regions form in the center of the inner and outer jets, in agreement with the findings of Ko and Kwan (1976) and Kwan and Ko (1977). For DNS2 ($r_u = 23.5$) the inner potential core does not exist due to the formation of a large recirculation region in $x/D_1 < 5$. In the present case the bubble encloses laminar flow and is in stationary motion, unlike Rehab *et al.* (1997) who observed a similar structures animated with solid body motion.

For both flows the Kelvin-Helmholtz instability in the inner and outer shear layers rolls up unto vortex rings organized in the form of an inner and outer helix structure. This corresponds to the development of an helical instability (mode $m = 1$) which agrees with the linear stability theory for a single jet, considering the ratio R/θ (Cohen and Wygnanski, 1987). It was observed that the inner rings are 'locked' into the outer ones, which due to their higher vorticity, impose their evolution upon the inner structures. It seems that the back-flow region has only a minor influence on this process until the end of the potential core (for DNS2). The frequency of the preferred mode for single (non-coaxial) jets, is well recovered in DNS1 ($r_u = 3.3$), but not in DNS2 ($r_u = 23.5$) due to the presence of the back-flow region which greatly complicates the flow downstream. In this case it was observed that the secondary structures (pairs of streamwise vortices) have unusually high values of vorticity modulus. This can be explained by the recirculation bubble which stretches these structures, thus being an additional source of axial vorticity production.

REFERENCES

Akselvoll, K. and Moin, P., 1996, "Large-eddy simulation of turbulent confined coannular jets", *J. Fluid Mech.*, Vol. 315, pp. 387-411.

Cohen, J. and Wygnaski, I., 1987, "The evolution of instabilities in the axisymmetric jet. Part 1. The linear growth of the disturbances near the nozzle", *J. Fluid Mech.*, Vol. 176, pp. 191-219.

Dahm, W. J. A., Friedler, C. E. and Tryggvason, G., 1992, "Vortex structure and dynamics in the near field of a coaxial jet", *J. Fluid Mech.*, Vol. 241, pp. 371-402.

Gutmark, E. and Ho, C.-M., 1983, "Preferred modes and the spreading rates of jets", *Phys. Fluids A*, Vol. 26, pp. 2932-2938.

Hunt, J. C. R., Wray, A. A. and Moin, P., 1988, "Eddies, stream, and convergence zones in turbulent flows", *Annual Research Briefs, Center for Turbulence Research, Stanford University.*

Ko, N. W. M. and Kwan, A. S. H., 1976, "The initial region of subsonic coaxial jets", *J. Fluid Mech.*, Vol. 73, pp. 305-332.

Kwan, A. S. K. and Ko, N. W. M., 1977, "The initial region of subsonic coaxial jets. Part 2", *J. Fluid Mech.*, Vol. 82, pp. 237-287.

Ko, N. W. M. and Chan, W. T., 1979, "The inner regions of annular jets", *J. Fluid Mech.*, Vol. 93, pp. 549-584.

Rehab, H., Villermaux, E. and Hopfinger, E. J., 1997, "Flow regimes of large-velocity-ratio coaxial jets", *J. Fluid Mech.*, Vol. 345, pp. 357-381.

Salvetti, M. V., 1996, "Numerical simulations of transitional axisymmetric coaxial jets", *AIAA J.*, Vol. 34, pp. 736-743.

Salvetti, M. V., 2000, "Effects of the velocity ratio on vorticity dynamics and mixing in coaxial jet flows", Proceedings, 1st Turbulent Shear Flow Phenomena.

da Silva, C. B., 2001, "The role of coherent structures in the control and interscale interactions of round, plane and coaxial jets", *PhD thesis, Institut National Politechnique de Grenoble.*

da Silva, C. B. and Métais, O., 2001, "Coherent structures in excited spatially evolving round jets", *DIRECT AND LARGE-EDDY SIMULATION IV, Kluwer Academic Publishers*

da Silva, C. B. and Métais, O., 2002, "Vortex control of bifurcating jets: a numerical study", *Phys. Fluids*, Vol. 14, pp. 3798-3819.

da Silva, C. B., Balarac, G., Begou P. and Métais, O., 2003, "Transition in high velocity ratio coaxial jets analysed from direct numerical simulations", *Journal of Turbulence* (in preparation).